JOURNAL OF CATALYSIS 92, 199–210 (1985)

# Investigation of the SMSI Catalyst $Pt/TiO_2$ by Small-Angle X-Ray Scattering

H. BRUMBERGER,* F. DELAGLIO,* J. GOODISMAN,* M. G. PHILLIPS,* J. A. SCHWARZ,† AND P. SEN†

*Department of Chemistry and †Department of Chemical Engineering and Materials Science, Syracuse University, Syracuse, New York 13210

Received May 24, 1984; revised October 16, 1984

Small-angle X-ray scattering measurements have been performed on $TiO_2$ supports and $Pt/TiO_2$ catalysts reduced at low and high temperatures, the latter exhibiting a strong metal–support interaction. For the supports the small-angle scattering yielded specific surface areas in good agreement with those from gas adsorption measurements, although with smaller error. To extract surface areas for the multiphase (support, metal, void) catalysts requires additional theory, developed here. In addition to scattering intensities for the catalyst, one uses the scattering intensities of a support which has undergone similar treatment (acidification, reduction, etc.). Metal surface areas considerably smaller than those deduced from electron micrographs of model catalysts are then calculated from the small-angle X-ray scattering. The free metal surface decreases by about ¼ in going from "normal" to SMSI catalyst, and this agrees well with electron microscopic observations. Temperature-programmed reduction, undertaken to gain information on the state of the metal, suggested the possible existence of PtO and $PtO_2$. If electron densities appropriate to these bulk phases are assumed in interpreting the X-ray scattering results, we find a much larger difference between "normal" and SMSI catalyst surfaces, however, than is suggested by electron micrographs. 

## INTRODUCTION

The discovery of the special properties of metals supported on titania by Tauster *et al.* (*1*), although not the first example of support influence on catalyst behavior, has led to hundreds of papers on "strong metal support interactions" (SMSI) in the last few years (*2–4*). A striking SMSI property is the suppression of $H_2$ and CO adsorption after reduction of the metal–support system at 773°K, and the return of the catalyst to its normal chemisorption behavior after oxidation and rereduction at 448°K. SMSI behavior has been investigated by a variety of techniques, and general ideas have emerged as to what factors can and cannot be responsible (*4*).

There is no appreciable agglomeration of Pt particles on high-temperature reduction, as evidenced (*5*) by the absence of X-ray Pt peaks, which implies that the particle size remains below about 2.5 nm. This rules out change in particle size as an explanation for the suppression of $H_2$ and CO chemisorption after high-temperature reduction. Other gross geometrical effects, such as massive sintering or encapsulation, were excluded by Tauster *et al.* (*1, 2*) on general grounds, such as the appearance of electron micrographs and the reversibility of the SMSI effect on oxidation, which can be done repeatedly. Baker *et al.* (*5*) found that this regeneration treatment produced an increase in Pt crystallite size. Resasco and Haller (*6, 7*) deduced from X-ray photoelectron and $H_2$ chemisorption results that some sintering occurred following the initial high-temperature reduction, but that particle sizes remained unchanged thereafter. That the SMSI effect was primarily electronic in origin was postulated early (*8*). There is a consensus that reduction of support, possibly catalyzed by Pt and Ir,



0021-9517/85 $3.00

alters the metal–support interaction, and is necessary to the effect. Residual hydrogen may also be important (*9–11*).

In this article, we apply the technique of small-angle X-ray scattering (SAXS) to the $Pt/TiO_2$ system. SAXS has been used to help characterize related catalyst systems, as it is a nondestructive method which can be applied to the commercial catalyst even in a working environment. This, however, appears to be the first application to an SMSI case. SAXS gives information about the various interphase surface areas in a multiphase system. It is consequently a very useful tool for SMSI catalysts in particular, since the SMSI effect on $H_2$ chemisorption emphasizes some limitations on the use of gas adsorption for surface area determination.

The general theory of SAXS has been extensively discussed elsewhere (*12, 13*); we consequently present, very briefly, only the basic relationships, and an extension of one of our scattering models to these complex four-phase catalysts. Details of the derivations and of some aspects of the scattering model may be found in Refs. (*12–15*).

## SMALL-ANGLE X-RAY SCATTERING

The scattered intensity $I(h)$ (where $h = 4\pi\lambda^{-1} \sin\theta$, $\lambda$ is the X-ray wavelength, $\theta$ is half the scattering angle) can be expressed as follows for a spatially isotropic scatterer:

$$I(h) = I_e(h) 4\pi V \overline{\eta^2} \int_0^\infty r^2 \gamma(r) \frac{\sin hr}{hr} dr. \quad (1)$$

Here,

$$I_e(h) = I_0 \left(\frac{e^2}{mc^2}\right)^2 \frac{1 + \cos^2 2\theta}{2l^2} \quad (2)$$

with $V$ the irradiated sample volume, $l$ the sample-detector distance, $I_0$ the primary intensity, and $(e^2/mc^2)^2$ the Thomson cross-section of the electron. $r$ is the scalar distance between pairs of scattering centers, $\overline{\eta^2}$ the mean-square electron density fluctuation in the sample, and $\gamma(r)$ is the correlation function, explicitly defined below. If the $n_i$ are the electron densities of the $i$ phases (support, void, metal), $\phi_i$ are their volume fractions, and $P_{ij}$ is the probability that $r$ lies with one end in phase $i$ and the other in phase $j$, then (*14*)

$$\eta_i = n_i - \bar{n} \quad (3)$$

$$\gamma(r) = 1 - \frac{\sum_{i>j} P_{ij}(n_i - n_j)^2}{\sum_i \phi_i (n_i - \bar{n})^2} \quad (4)$$

$$\overline{\eta^2} = \overline{n^2} - \bar{n}^2 = \overline{n^2} - \left(\sum_i \phi_i n_i\right)^2. \quad (5)$$

For experimental conditions employing "infinite slit" optics (*16*), it may be shown (*12*) that

$$\tilde{Q} = \int_0^\infty h\tilde{I}(h)\, dh = 4\pi^2 I_e(h) V \overline{\eta^2}. \quad (6)$$

The tilde over the various quantities refers to "infinite slit" measurements.

For models with internally homogeneous phases and sharp electron-density transitions at phase boundaries, the interfacial areas $S_{ij}$ are related to the $P_{ij}$ (*13, 14*):

$$\frac{S_{ij}}{4V} = \left(\frac{dP_{ij}}{dr}\right)_{r=0} \quad (7)$$

and thus

$$\gamma'(0) = -\frac{1}{4V} \sum_{i>j} \frac{S_{ij}(n_i - n_j)^2}{\overline{\eta^2}}. \quad (8)$$

For systems with well-defined internal surfaces (*13*)

$$\lim_{h\to\infty} h^3 \tilde{I}(h) = \tilde{k} = -4\pi^2 I_e(h) \overline{\eta^2} V \gamma'(0) \quad (9)$$

where $\gamma'(0)$ is the first derivative of the correlation function, evaluated at the origin. $\gamma'(0)$ may then be found from the experimentally accessible parameters $\tilde{k}$ and $\tilde{Q}$:

$$\gamma'(0) = -\tilde{k}/\tilde{Q}. \quad (10)$$

Thus a connection between these and the $S_{ij}$ is established.

For a two-phase system, $\tilde{k}/\tilde{Q}$ gives $S_{21}$ directly; there is only one independent probability, $P_{21}$, and one surface (*17*):

TABLE 1

Phase Properties

| | Phase | Mass density (g $cm^{-3}$) | Electron density, $n_i$ (mole $cm^{-3}$) |
|---|---|---|---|
| 1 | Anatase | 3.84 | 1.826 |
| 2 | Rutile | 4.26 | 2.026 |
| 3 | Void | 0.0 | 0.0 |
| 4 | Platinum | 21.45 | 8.576 |
| | PtO | 14.9 | 6.070 |
| | $PtO_2$ | 10.2 | 4.222 |

$$\gamma'(0) = \frac{-S_{21}}{4V\phi_1\phi_2}. \qquad (11)$$

Only the volume fractions, which are calculable from density measurements, are needed. Our titania supports,[1] however, are not true two-phase systems because they are composed of anatase (electron density $n_1 = 1.826$) and rutile (electron density $n_2 = 2.026$) in a ratio of 4 to 1 by weight (Table 1). As shown in the Appendix, because of the small density contrast between phases 1 and 2, $S_{21}$ hardly contributes unless the dispersity of phases 1 and 2 among themselves is orders of magnitude higher than of either against the void ($S_{21} \gg S_{31}$ or $S_{32}$). The ratio of volume fractions $\phi_1/\phi_2$ is 4.438, and the ratio of $S_{31}$ to $S_{32}$ will be roughly $\phi_1/\phi_2$. The support is thus considered as a two-phase system, with a single surface, $S_{31} + S_{32}$. (Our catalyst is actually 4-phase, but assuming that the titania can be treated as a single phase makes it 3-phase.)

For a general $N$-phase system, there are $\frac{1}{2}N(N-1)$ surface areas (*14*) and $\frac{1}{2}N(N-1)$ surface-to-volume ratios, whereas $\tilde{k}/\tilde{Q}$ represents a single experimentally determined intensive parameter of the system. To get the surface areas for the catalyst systems from $\gamma'(0)$ requires additional assumptions about the catalyst areas and about the relation of catalyst to support. We assume that the titania in a catalyst is identical to the metal-free titania support which has undergone the same treatment (including acidification, heating, but not impregnation with platinum) as the catalyst. The fact that X-ray powder patterns for titania are the same in the support thus treated and in the catalyst implies that there are no gross differences between the two. This makes it possible to subtract, essentially, the support contribution to the scattering in order to obtain the specific surface contribution of the metal. A detailed treatment of a similar scattering model and of its assumptions has been given previously for three-phase systems (*15*). The extension to four phases is shown in the Appendix, where any additional or different assumptions are also noted.

The advantage of this SAXS approach, and an important difference from some earlier SAXS investigations of catalysts (*18–20*), is that it does not require the use of imbibition liquids, or other relatively drastic procedures, to mask the pore scattering. Imbibition liquids may affect the catalyst in unknown ways, and it is difficult to fill the pores with them reproducibly.

Small-angle X-ray scattering measurements were carried out on two samples of catalyst (titania impregnated with platinum), and two samples of the support (titania) which had all been freshly reduced and stored in screw-cap vials in air. The two catalyst samples differed in their reduction temperatures, 448 and 773°K, corresponding to normal and SMSI behavior. The support samples were acid treated before being reduced, one at 448 and one at 773°K. The acid treatment was to reproduce the treatment at the pH of the platinum impregnation step of catalyst preparation. Indeed, this treatment changed the physical properties of the support: it gave it a blue color and reduced the caking tendency observed for the untreated support which, incidentally, made density measurements on the latter unreliable.

The X-ray scattering of the powder samples was measured with a Kratky small-an-

[1] We are indebted to Dr. S. J. Tauster for furnishing the support and catalyst samples.

TABLE 2

Measured Parameters from Small-Angle X-Ray Scattering

| Sample | $\tilde{k}/\tilde{Q}$ ($nm^{-1}$) |
|---|---|
| Support reduced at 448°K | 0.0608 ± 0.0001 |
| Support reduced at 773°K | 0.0597 ± 0.0003 |
| Catalyst reduced at 448°K | 0.0663 ± 0.0007 |
| Catalyst reduced at 773°K | 0.0631 ± 0.0004 |

gle camera in the "infinite slit" geometry (*16*). Instrumental background corrected for sample absorption was subtracted from all scattering curves. From the resulting sample scattering curve, $\tilde{I}(h)$ vs $h$, a plot of $h^3\tilde{I}(h)$ was generated, from which the limiting value $\tilde{k}$ was obtained. The $h\tilde{I}(h)$ vs $h$ curve has an experimentally accessible maximum, so that this function can be extrapolated to the origin with reasonable confidence. From a value $h = H$, the intensity drops as $\tilde{k}/h^3$. Thus $\tilde{Q}$ can be found by numerical integration of $h\tilde{I}(h)$ vs $h$ in the interval $0 \leq h < H$, and analytically in the interval $H \leq h \leq \infty$:

$$\int_H^\infty h\tilde{I}(h)\, dh = \tilde{k}/H. \qquad (12)$$

Table 2 gives the results of the small-angle scattering measurements as values of $\tilde{k}/\tilde{Q}$. The precision given is the average deviation of 3–4 repeated measurements.

According to the discussion in the Appendix, for support approximated as a two-phase system,

$$\frac{\tilde{k}}{\tilde{Q}} = \frac{(S_{32} + S_{31})}{4V\phi_s(1 - \phi_s)} \qquad (13)$$

where $S_{32} + S_{31}$ is the sum of anatase-void and rutile-void surface areas and $\phi_s$ is the total volume fraction of titania. The two supports give quite similar $\tilde{k}/\tilde{Q}$ values, although that found for the high-temperature samples is slightly smaller. The same is true for the two catalysts. However, there is an increase in $\tilde{k}/\tilde{Q}$ in going from either support to the corresponding catalyst. The difference in $\tilde{k}/\tilde{Q}$ for two samples of identical composition reflects a difference in surface areas; the difference between samples of different composition involves changed electron densities as well.

### *1. Support Surfaces*

To derive surface areas from the SAXS measurements on the support, we need $\phi_s$, the volume fraction of solids (anatase + rutile), which can be obtained from the bulk density of the support. To obtain $\phi_s$, the density obtained from mercury displacement measurements at 1 atm pressure ($\rho_1$) was combined with mercury porosimetry measurements[2] for pressures from 1 to 3 × $10^4$ psi. The bulk density at 0 pressure, $\rho_0$, was calculated according to $(1/\rho_0) = (1/\rho_1) + \Delta V$, where $\Delta V$ is the difference between intrusion volumes per gram at 1 atm and at 0 pressure. The result is 0.851 g $cm^{-3}$. From the anatase and rutile densities (Table 1) we calculate a skeletal density of 3.9172 g $cm^{-3}$, so that $\phi_s = 0.2173$ and the anatase and rutile volume fractions are 0.1773 and 0.0400, respectively. For the two supports, Eq. (13) then gives $S/V = 0.0414$ and 0.0406 $nm^{-1}$. To convert these values to specific surfaces, we multiply by $10^3/\rho$, $\rho$ being the density in g $cm^{-3}$. With $\rho = 0.851$, we find 48.6 and 47.7 $m^2\ g^{-1}$ for the support samples reduced at 448 and 773°K, respectively. These agree quite well with the BET results reported by Tauster: 50 ± 15 $m^2\ g^{-1}$ for an untreated support and 43 $m^2\ g^{-1}$ for a support reduced at 773°K. The precision of the X-ray results, however, is considerably better.

The difference in $\tilde{k}/\tilde{Q}$ values and hence in surface areas for the supports reduced at different temperatures is 1.8% which is only slightly above the precision of the measurements (about 1%). Small-angle measurements on support reduced at 773°K but *not* acid-treated (this sample remained white instead of developing a blue color like

[2] The porosimetry measurements were obtained by Porous Systems, Inc., Ithaca, N.Y.

TABLE 3

Calculated $S_{43}^{(4)}/V$ in $nm^{-1}$ for Free-Metal Surface as a Function of $r$ for Two Catalysts

| $r$ | $S_{43}^{(4)}/V \times 10^4$ (448°K) | $S_{43}^{(4)}/V \times 10^4$ (773°K) |
|---|---|---|
| 1.0 | 2.373 | 1.881 |
| 2.0 | 2.896 | 2.296 |
| 3.0 | 3.126 | 2.478 |
| 5.0 | 3.337 | 2.646 |
| 8.0 | 3.470 | 2.751 |
| 12.0 | 3.548 | 2.813 |
| ∞ | 3.715 | 2.946 |

the others) gave $\tilde{k}/\tilde{Q} = 0.058\ nm^{-1}$, substantially different from the values found for acid-treated support. Since densities could not be determined reliably for the untreated $TiO_2$ because of caking, specific surfaces were not calculated. Acid treatment apparently helps to break up the solid matrix.

*2. Metal Surfaces*

According to Eqs. (A4) and (A5) of the Appendix, with $\phi_1^{(4)}/\phi_2^{(4)} = 4.438$, the metal-void surface $S_{43}^{(4)}$ of the catalyst is given by

$$-\frac{S_{43}^{(4)}}{4V} = 5.438\, r\, \frac{[\overline{\eta^2}\gamma'(0)]^{(3)} - [\overline{\eta^2}\gamma'(0)]^{(4)}}{[4.438(2n_1n_4 - n_4^2 - rn_4^2) + 2n_2n_4 - n_4^2 - rn_4^2]} \tag{14}$$

The subscripts 1 and 2 refer to the two support phases (anatase and rutile), 3 is the void, 4 the metal. Superscripts refer to the four-phase catalyst and three-phase support. The parameter $r$ is the ratio of free to covered surfaces of the catalyst, i.e.

$$r = \frac{S_{43}^{(4)}}{S_{41}^{(4)} + S_{42}^{(4)}}. \tag{15}$$

Using the electron density of metallic platinum for $n_4$ and the fact that the catalyst is 2% Pt by weight so that $\phi_{Pt} = 0.00081$, we have $\overline{\eta^2} = 0.645$ for the 4-phase system and $\overline{\eta^2} = 0.591$ for the 3-phase system. Then the above equation becomes

$$\frac{S_{43}^{(4)}}{V} = r\, \frac{0.645[\gamma'(0)]^{(4)} - 0.591[\gamma'(0)]^{(3)}}{-10.40 - 18.39r} \tag{16}$$

which gives $(2692 + 1522/r)^{-1}\ nm^{-1}$ for the low-temperature catalyst and support, and $(3395 + 1920/r)^{-1}\ nm^{-1}$ for the high-temperature catalyst and support. As a function of $r$, the results are presented in Table 3. The insensitivity to $r$ for $r > 3$ is shown. A surface-to-volume ratio of $2.300 \times 10^{-4}\ nm^{-1}$, for example, corresponds to 0.284 $nm^2$ of surface per $nm^3$ of metal. For hemispherical particles ($r = 2$), this implies an average radius of 10.6 nm.

The transmission electron micrographs of Pt particles on $TiO_2$ films (*5, 21*) showed that the average Pt particle diameter increased from about 2.5 to about 5 nm when the system was heated above 825°K in $H_2$. [Lehn *et al.* (*22*) deduced Pt particle diameters of 3 nm for their $Pt/TiO_2$ catalysts, which were ~4% Pt.] Further, the particles changed from hemispherical to raft-like. The spreading to structures less than 2 nm thick, together with the catalytic effect on $TiO_2$ reduction, was taken to indicate a strong chemical interaction between metal and substrate, as was the fact that the particle size distribution on $TiO_2$ was more stable to temperature and other factors than the size distribution on other supports ($Al_2O_3$, $SiO_2$, C). Hemispherical Pt particles of diameter $d$ nm have a free surface area of $\frac{1}{2}\pi d^2$ $nm^2$ and a mass of $21.45 \times 10^{-21}$ ($\pi d^3/12$) g, so the free Pt surface per unit volume of catalyst (using 0.851 g $cm^{-3}$ as the support bulk density and 2% metal loading) is (0.2797) (0.868)(0.02)/$d$ $nm^{-1}$. If $d$ is taken as 2.5 nm, $1.94 \times 10^{-3}\ nm^{-1}$ is found for the Pt area per unit catalyst volume. Pillbox-shaped rafts of thickness 1 nm and diameter $d$ nm would have a free Pt surface area per unit volume of catalyst of $(21.45)^{-1}$ $(1 + 4/d)$ (0.868) (0.02) $nm^{-1}$, which, for $d = 5$ nm, gives $S/V = 1.46 \times 10^{-3}\ nm^{-1}$. These areas are much larger than those we obtained from SAXS. The samples used in the electron microscopic

and SAXS studies were of course very different. The former were prepared by evaporation of Pt onto a model support film, the latter by impregnating a $TiO_2$ powder support with solutions of chloroplatinic acid and subsequent calcination and reduction. It is, therefore, not unexpected that substantial differences would arise in the absolute values of the surface areas. It is, however, significant that the decrease in areas by about $\frac{1}{4}$ in going from the low- to the high-temperature catalyst agrees with our SAXS results. The calculated metal-void surface areas increase markedly if a much lower electron density is used for the Pt-bearing phase. We have so far assumed that the Pt is in metallic form. It is well known that PtO and $PtO_2$ do not form readily from Pt under ordinary conditions; the preparation of PtO calls for heating Pt to 693°K under 8 atmospheres of $O_2$ (*23*), and preparation of $PtO_2$ involves heating Pt to 723°K in 150 atm of $O_2$, which gives a mixture of Pt, PtO, and $PtO_2$, from which the Pt and PtO are dissolved away using aqua regia. Ignition of Pt at 1273–1673°K in air or oxygen forms $PtO_2$, but it is "unstable at low temperatures, decomposing readily even at 380–400°C (*24*)." The hydrated compound may be prepared from Pt IV salts, but complete dehydration occurs simultaneously with decomposition to Pt + $O_2$ (*24*). On the other hand, the equilibrium for the reaction of Pt(s) and $O_2$ to $PtO_2$ is shifted to the right at higher temperature (*25*), so that $PtO_2$ formation is responsible for the loss of Pt from the Pt gauze catalyst used in air oxidation of $NH_3$ at 1 atm pressure and a temperature of 1123°K. Surface oxides or other compounds on Pt have also been suggested (*26*) on the basis of NMR measurements.

The weight losses measured by temperature-programmed reduction (discussed in the following section) do at least raise the possibility that the platinum may actually be present as oxides. With the same experimental X-ray data (Table 2) we have therefore also calculated surface areas according to (A5) using densities $n_4$ appropriate to the oxides rather than Pt (Table 1). In each case, $S_{43}^{(4)}/V$ is written in the form

$$S_{43}^{(4)}/V = (a + b/r)^{-1}. \qquad (17)$$

The coefficients $a$ and $b$ are tabulated, for various possible Pt phases, in Table 4. In Table 5, we have shown how the free surface, $S_{43}^{(4)}$, calculated from the scattering data for the platinum-bearing phase, depends on the changed assumption for its electron density. For this illustration, values of $S_{43}^{(4)}$ have been calculated for $r = \infty$, so that they represent the maximum values for this surface, and converted to $m^2$ per gram of catalyst. The metal-support surface is given by $S_{41}^{(4)} + S_{42}^{(4)}$, with the assumption that $S_{41}^{(4)}/S_{42}^{(4)} = \phi_1^{(4)}/\phi_2^{(4)}$, so that

$$S_{ms} = S_{43}^{(4)}/r = V(a + b/r)^{-1}r^{-1}. \qquad (18)$$

Here, "m" and "metal" refer to the platinum-bearing phase. The surface $S_{ms}$ is more sensitive than $S_{43}^{(4)}$ to the value of $r$ when $r$ is large, becoming zero as $r$ becomes infinite.

TABLE 4

Effect of Changing Platinum Phase

| Pt phase | Volume fraction $\phi_4$ | $\overline{\eta^{2(4)}}$ | Low-temp. coeffs.[a] | | High-temp. coeffs.[a] | |
|---|---|---|---|---|---|---|
| | | | $a$ | $b$ | $a$ | $b$ |
| Pt | 0.000809 | 0.6448 | 2692 | 1522 | 3395 | 1920 |
| PtO | 0.001261 | 0.6312 | 1555 | 601 | 2023 | 781 |
| $PtO_2$ | 0.001981 | 0.6194 | 867 | 102 | 1170 | 138 |

[a] The surface-to-volume ratio in $nm^{-1}$ is given by $S/V = (a + b/r)^{-1}$.

TABLE 5

Platinum Surface Areas in $m^2\ g^{-1}$ Catalyst[a]

| Pt phase | Low-temperature reduction | | High-temperature reduction | |
|---|---|---|---|---|
| | $S_{43}^{(4)}$ | $S_{41}^{(4)} + S_{42}^{(4)}$ | $S_{43}^{(4)}$ | $S_{41}^{(4)} + S_{42}^{(4)}$ |
| Pt | 0.428 | 0.120 | 0.339 | 0.095 |
| PtO | 0.741 | 0.219 | 0.569 | 0.168 |
| $PtO_2$ | 1.329 | 0.426 | 0.985 | 0.316 |

[a] $S_{43}^{(4)}$ for $r = \infty$, $S_{41}^{(4)} + S_{42}^{(4)}$ for $r = 3$.

The values in Table 5 are for $r = 3$. The fact that it is about $\frac{1}{3}$ the maximum value of $S_{43}^{(4)}$ reflects the insensitivity of $S_{43}^{(4)}$ to the value of $r$.

## TEMPERATURE-PROGRAMMED REDUCTION

We have indicated the importance of knowing the electron densities of the phase in the multiphase catalyst system for interpreting the SAXS measurements. Evidence from the literature (*27*) indicates that the method of catalyst preparation, including the choice of metallic salt, the drying, the duration and temperature of calcination, and the choice of support can affect the oxidation state of the dispersed metal. Temperature-programmed reduction (TPR) offers the possibility of determining the oxidation state of catalyst (*28*) and such experiments may therefore help to interpret the SAXS results. The results reported below were obtained from aliquots of identically prepared $Pt/TiO_2$ catalysts, where the only difference in the final step of their preparation was the reduction temperature. Therefore differences in results represent the effect of reduction temperature on the oxidation state of the metal or support.

Temperature-programmed reduction was carried out in a Cahn vacuum microbalance, model RG2. The balance has a maximum sensitivity of 0.3 $\mu$g; complete specification of the balance and the grease-free high vacuum system can be found elsewhere (*29*). The experimentally determined quantity is the weight loss as a function of temperature. The derivative of these experimental results yields the temperature-programmed reduction spectrum. For the purpose of comparison, the data will be displayed in this form, although the quantitative results are based on direct measurement of the weight loss. Several temperature-programmed reductions in hydrogen, of ultrahigh purity and further purified by an oxidation catalyst and molecular sieve trap, were obtained for these catalyst samples. The three samples were the pretreated support (see below), $Pt/TiO_2$ reduced at 448°K (normal catalyst) and $Pt/TiO_2$ reduced at 773°K (SMSI catalyst). The Degussa $TiO_2$ was subjected to acidification in HCl at pH ~ 2.5, corresponding to the pH of a solution of hexachloroplatinic acid with a concentration required to deposit 2% by weight onto the $TiO_2$ support. This was followed by calcination at 773°K. In all cases, the samples were dehydrated *in situ* in a flow of ultrahigh purity helium (100 $cm^3$ $min^{-1}$) during temperature programming from room temperature to 773°K at 5°K $min^{-1}$. It is interesting to note that the as-received support and acidified support showed substantially different temperature-programmed reduction spectra. The weight loss as a function of temperature for the acidified support was used as a background and was subtracted from the results for the supported metal catalysts. This correction was small compared to the weight loss on reduction of the catalysts.

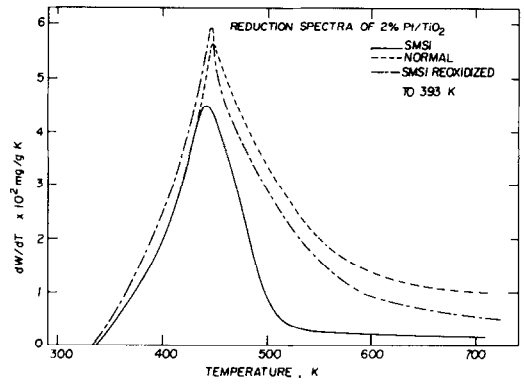


FIG. 1. Weight losses during temperature-programmed reduction of several $Pt/TiO_2$ catalysts.

Figure 1 shows the temperature-programmed reduction spectra for "normal" and SMSI catalysts. For the normal catalyst (initially reduced at 448°K) the temperature programming in hydrogen was extended to 773°K. The reduction spectra of both catalysts show a peak at ~448°K; the normal catalyst shows a substantially higher peak and a long tail that continues to 773°K. The latter effect could be attributed to reduction of the support via a hydrogen

spillover mechanism. The data on weight loss vs temperature were used to determine directly the total weight loss.

The results for the normal catalyst are difficult to interpret because the weight loss continued at an appreciable rate until the cessation of heating at 773°K. However, the data for the SMSI catalyst show that reduction is nearly complete by ~523°K. For a sample of 2% Pt on titania containing 100 $\mu$mole of Pt metal, the amount of water formed during temperature-programmed reduction of the SMSI catalyst was 93 $\mu$mole (210 $\mu$mole was formed from a sample of normal catalyst containing the same amount of Pt). Auxiliary experiments in another apparatus with an on-line mass spectrometer showed that water was the only gas-phase product. Quantitative determination of the amount of water produced was difficult due to condensation in the vacuum system, so that these results were only qualitative compared to those obtained from the microbalance studies.

The magnitude of the absolute weight loss for the SMSI catalyst would be consistent with reduction of the metal, if it is in the form of bulk PtO and if no support reduction occurs. For the normal catalyst, the weight loss (which can only be considered approximate due to the tail in the TPR curve) would correspond to $PtO_2$ under corresponding circumstances. This, however, is not compatible with thermodynamic evidence. The possibility that these effects are due to reduction of the supports appears more reasonable. However, this then raises the question of why the amount of water is comparable, on a mole basis, to the amount of platinum, when there is excess support compared to the amount of metal present. During reduction water is released and water is a known cocatalyst for enhancement of hydrogen spillover (*30*). If such mechanisms are operating, these facts suggests that the water loss during reduction involves an intimate mixture of Pt and $TiO_2$.

We also tested the conclusions reached by Tauster *et al.* (*1*) that SMSI catalysts could be transformed to normal catalysts by recalcination followed by reduction at 448°K. In Fig. 1 the intermediate curve was obtained after the normal catalyst was subjected to the procedures of temperature-programmed reduction which should render it SMSI (773°K in flowing hydrogen). Subsequent to this several different samples were calcined at 393°K for 1 hr. The results of temperature-programmed reduction of these catalysts showed an intermediate behavior.

## DISCUSSION AND CONCLUSIONS

We have demonstrated the utility and limitations of small-angle X-ray scattering as a tool for investigation of catalyst systems. It is possible to monitor samples as temperature or chemical environment is changed. In principle, SAXS gives the information necessary for calculating several interfacial areas simultaneously, irrespective of their chemical nature. BET and related methods depend on the availability of a suitable adsorbing gas which can contact all of the surface to be measured, and whose adsorption behavior is known. The existence of the SMSI effect itself affords a striking example of a problem with gas adsorption: hydrogen adsorption would give quite false values for the platinum surfaces for $Pt/TiO_2$ reduced at high temperatures. On the other hand, a combination of gas adsorption measurements with SAXS measurements can give interesting information about the nature of the surfaces.

As we have shown, to derive surface areas from the SAXS measurements, volume fractions and electron densities of the phases are required. The former are readily obtained from density measurements and from assays of the catalyst. The electron density of a phase is simply calculated from its mass density, provided the chemical nature of the phase is known. Temperature-programmed reduction is one technique which may give this information. Nuclear magnetic resonance and ion sputtering are others. We have shown that changed as-

sumptions about the nature of the phase (e.g., PtO or $PtO_2$ instead of Pt) lead to quite different values for surface areas. However, changes of several percent in electron density, due to the kinds of electron transfer from support discussed in the preceding sections, are not important enough to affect SAXS surface areas.

There is little ambiguity in the support surface area derived from SAXS. In the case of a two-phase system, the analysis is simple and the value of the single interphase surface area is insensitive to the density. Thus the values we report for the $TiO_2$/void surface of the unmetallized support should be quite reliable. These agree with BET results, which, however, are not as precise. Our results show a significant difference between untreated and acid-treated support, accompanying other physical changes on acidification. In contrast, supports reduced at low and high temperature have identical surface areas within the accuracy of the SAXS technique.

Addition of platinum leads to a significant change in the X-ray scattering curve. Assuming the support in the catalyst has the same geometric properties as the unmetallized support, we have derived free surface areas for Pt considerably smaller than those derived from interpretation of electron micrographs for related model (thin film) systems. Our theory still involves a parameter $r$, whose value, however, turns out to affect the free metal surface little. It has a large effect on the metal–support surface area. Since $r$ is dependent on Pt particle shape, information on its value could come from electron micrographs. The metal surface areas calculated from SAXS measurements are subject to uncertainties related to the scattering model and to the electron densities assumed for the phases. Small changes, such as that due to reduction of a small fraction of support, or an increase of several percent in the Pt $d$-band density, are not a problem. As seen above, however, the assumption of bulk PtO or $PtO_2$ for the metal-containing phase leads to much higher calculated surface areas. Thus TPR, XPS, and other methods for ascertaining the oxidation state of Pt may furnish important auxiliary information.

Temperature-programmed reduction was carried out on normal and SMSI catalysts. The 2 : 1 ratio of weight losses found suggests that the metal phases may be oxides. Assuming PtO for the SMSI catalyst and $PtO_2$ for the "normal" catalyst, we calculate (cf. Table 4) free surface areas for the metal-bearing phase of $4.0702 \times 10^{-4}$ and $10.893 \times 10^{-4}$ $nm^{-1}$, respectively. (We have taken $r = 2$, appropriate for hemispheres, for the low-temperature catalyst, and $r = 1.8$, appropriate for rafts of diameter 5 nm and thickness 1 nm, for the other.) While the larger values approach those derived from electron micrographs, the increase of surface area by a factor of ~2.7 from SMSI to normal catalyst is far too large compared with what is observed in electron microscopic studies. We tend, therefore, to believe that the bulk Pt-bearing phase is metallic platinum.

The question then becomes one of reconciling the SAXS results, which, taking Pt to be the metallic phase, yield reasonable relative free metal surface areas for "normal" and SMSI catalysts, to the TPR data. Huizinga and Prins (*31*) have reported encapsulation of Pt after treatment of $Pt/TiO_2$ above 1013°K, which results in the anatase–rutile phase transformation. It has also been suggested that, although complete encapsulation does not occur, there is some covering of the metal by support in passing to the SMSI state. Evidence for migration of a reduced Ti species $TiO_x$ over the metal in the case of high-temperature reduced $Rh/TiO_2$ came (*7, 32*) from Auger and argon-ion sputtering (Ti and Rh profiles). EXAFS on the sample after high-temperature reduction showed an increase in the number of Rh–O neighbors, which could be interpreted in terms of migration. However, an increase in the number of Pt–O neighbors for $Pt/TiO_2$ was not found.

Herrmann, Disdier, and Pichat (*33*), from

measurements of electrical conductivity and photoconductivity of $TiO_2$ and $Pt/TiO_2$, suggested that H atoms could be transferred from metal to support and electrons from anatase to metal, which would make Pt behave more like Au. The change in electron density, however, would not be important for the interpretation of our X-ray results. From EXAFS and X-ray absorption edge measurements it appears (*34*) that Pt on $TiO_2$ has 0.04 more vacant *d* states per atom than bulk Pt, with a slight but significant decrease in this figure for the high-temperature reduced catalyst. It is also found that Pt–Pt distances in $Pt/TiO_2$ are smaller than those in bulk Pt or $Pt/SiO_2$; the decrease is more important for higher reduction temperatures. No evidence for stronger Pt–O interactions was found. Tauster *et al.* (*2*) proposed a model for SMSI in which Ti–Pt bonding involving cation *d*-orbitals gives a negative charge to Pt and hence an increase in electron density on Pt supported on $TiO_2$. Changes in electron density of a few percent would affect our X-ray results very little, nor would a very thin film of a titanium oxide on the surface of the platinum. It is possible, however, that reduction of oxygen chemisorbed on Pt, or of surface platinum oxides, together with support material which covers the Pt with a thin layer, can account for the observed TPR results.

## APPENDIX: THEORY OF SAXS FOR MULTIPHASE SUPPORTED-METAL CATALYSTS

To extract surface areas for supported-metal catalysts from $\tilde{k}/\tilde{Q}$ we must deal with two problems: the fact that the support is not really a two-phase system and the fact that the catalyst itself involves at least three surfaces. Considering the support as a 4 : 1 anatase–rutile mixture, we have, according to Eqs. (*4*) and (*8*), using the electron densities of Table 1:

$$-4V\gamma'(0) = (3.334S_{31} + 4.105S_{32} + 0.040S_{21})/\overline{\eta^2}. \quad \text{(A1)}$$

If $S_{21}$ is not orders of magnitude larger than the other surfaces, the term in $S_{21}$ can be dropped. Further, we expect that the ratio of $S_{31}$ to $S_{32}$ will be essentially the ratio of volume fractions $\phi_1$ to $\phi_2$, leaving only one independent surface. Dropping the $S_{21}$ term makes $-4V\gamma'(0)$ equal to $18.901\, S_{32}/\overline{\eta^2}$. Further, $\bar{n} = 1.826\phi_1 + 2.026\phi_2 = 1.863\phi_s$ and $\overline{\eta^2} = 3.476\phi_s - (1.863\phi_s)^2$, where $\phi_s$ is the total titania volume fraction, so $-4V\gamma'(0)$ is essentially $(S_{31} + S_{32})/\phi_s(1 - \phi_s)$. The support is effectively a two-phase system, with a solid phase with average electron density 1.863 mole $cm^{-3}$ (weighted mean of anatase and rutile) and total surface area $S_{31} + S_{32}$ (weighted roughly in the same way).

Turning to the catalyst, we note that even for a true two-phase (solid, void) support and a three-phase (solid, void, metal) catalyst the two values of $\tilde{k}/\tilde{Q}$ would not suffice to determine three independent specific surfaces. However, we will see that a meaningful value for the metal-void surface can still be derived. We will give our formulae for the full system (three-phase support, four-phase catalyst) so that all the assumptions appear (compare Ref. (*15*)). The electron densities are $n_i$ ($i = 1 \ldots 4$). Superscripts (3) and (4) distinguish results for support (three phases) and catalyst (four phases), respectively. Finally, $Q_{ij}$ represents $-P'_{ij}(0)$, which is $-S_{ij}/4V$. Then we have

$$[\overline{\eta^2}\gamma'(0)]^{(3)} = Q_{21}^{(3)}(n_1 - n_2)^2 + Q_{31}^{(3)}(n_1 - n_3)^2 + Q_{32}^{(3)}(n_2 - n_3)^2 \quad \text{(A2)}$$

and

$$[\overline{\eta^2}\gamma'(0)]^{(4)} = Q_{21}^{(4)}(n_1 - n_2)^2 + Q_{31}^{(4)}(n_1 - n_3)^2 + Q_{41}^{(4)}(n_1 - n_4)^2 + Q_{32}^{(4)}(n_2 - n_3)^2 + Q_{42}^{(4)}(n_2 - n_4)^2 + Q_{43}^{(4)}(n_3 - n_4)^2. \quad \text{(A3)}$$

Equations (A2) and (A3) involve nine unknown quantities and only two measured parameters.

The support being unchanged on metallization, $Q_{21}^{(3)} = Q_{21}^{(4)}$. Since the metal is deposited on the free surface of support,

$$Q_{31}^{(3)} = Q_{31}^{(4)} + Q_{41}^{(4)}$$

and

$$Q_{32}^{(3)} = Q_{32}^{(4)} + Q_{42}^{(4)}.$$

If the two support phases have the same dispersity,

$$Q_{31}^{(3)}/Q_{32}^{(3)} = \phi_1^{(3)}/\phi_2^{(3)}$$
$$Q_{31}^{(4)}/Q_{32}^{(4)} = \phi_1^{(4)}/\phi_2^{(4)}$$
$$Q_{41}^{(4)}/Q_{42}^{(4)} = \phi_1^{(4)}/\phi_2^{(4)}$$

where $\phi_1^{(3)} = \phi_1^{(4)}$, $\phi_2^{(3)} = \phi_2^{(4)}$, and $\phi_3^{(3)} = \phi_3^{(4)} + \phi_4^{(4)}$. Of course these are not all independent; the third, which is the only one we use, follows from the other two. We introduce the parameter

$$r = Q_{43}^{(4)}/(Q_{41}^{(4)} + Q_{42}^{(4)})$$

whose value and significance will be discussed later. Subtracting (A3) from (A2), we obtain

$$\begin{aligned}[\overline{\eta^2}\gamma'(0)]^{(3)} - [\overline{\eta^2}\gamma'(0)]^{(4)} &= Q_{41}^{(4)}(n_1 - n_3)^2 + Q_{42}^{(4)}(n_2 - n_3)^2 \\ &\quad - Q_{41}^{(4)}(n_1 - n_4)^2 - Q_{42}^{(4)}(n_2 - n_4)^2 \\ - Q_{43}^{(4)}(n_3 - n_4)^2 &= [(n_1 - n_3)^2 - (n_1 - n_4)^2 \\ &\quad - r(n_3 - n_4)^2]Q_{41}^{(4)} + [(n_2 - n_3)^2 \\ &\quad - (n_2 - n_4)^2 - r(n_3 - n_4)^2]Q_{42}^{(4)} \\ &= Q_{41}^{(4)}\left[2n_1n_4 - n_4^2 - rn_4^2 + \frac{\phi_2^{(4)}}{\phi_1^{(4)}} \right. \\ &\quad \left. \times (2n_2n_4 - n_4^2 - rn_4^2)\right]. \quad \text{(A4)}\end{aligned}$$

We have simplified the last group of equations by noting that $n_3$ vanishes.

The metal-void surface (free metal surface) is of particular interest; it is given by $4VQ_{43}^{(4)}$, where

$$Q_{43}^{(4)} = r(Q_{41}^{(4)} + \phi_2^{(4)}Q_{41}^{(4)}/\phi_1^{(4)}). \quad \text{(A5)}$$

Combining with (A4), we get $Q_{43}^{(4)}$; other metal surfaces can likewise be calculated. Equations (A3) and (A4) show that knowledge of $\gamma'(0)$ for the three- and four-phase systems, together with volume fractions (obtained from density measurements), and a value for $r$ give the metal-void surface. The parameter $r$ is the ratio between free and covered (in contact with support) metal surfaces. It would be unity for extended metal layers, with lateral area negligible compared to top surface, and infinity in the limit of metal spheres touching the support at a point only. For hemispherical caps of radius $R$, $r = 2$; for tetrahedra $r = 3$; for cubes $r = 5$. For a right cylinder of height $H$ and width $W$ to have $r < 3$ would require $H < W/2$. As shown in Table 5, the value of $r$ is not too important in determining $S_{41}^{(4)}$ as long as it is not too near unity.

ACKNOWLEDGMENTS

This work was supported by the National Science Foundation under Grant CPE-7913779. J.A.S. acknowledges support for manuscript preparation from Grant DE-AC02-84ER 13158.

REFERENCES

1. Tauster, S. J., Fung, S. C., and Garten, R. L., *J. Amer. Chem. Soc.* **100,** 170 (1978).
2. Tauster, S. J., Fung, S. C., Baker, R. T. K., and Horsley, J. A., *Science* **211,** 1121 (1981).
3. Imelik, B. *et al.* (Eds.), "Metal-Support and Metal-Additive Effects in Catalysis." Elsevier, Amsterdam, 1982.
4. Bond, G. C., and Burch, R., *Spec. Period. Rep. Catal.* **6,** 27 (1983).
5. Baker, R. T. K., Prestridge, E. B., and Garten, R. L., *J. Catal.* **59,** 293 (1979).
6. Resasco, D. E., and Haller, G. L., *Appl. Catal.* **8,** 99 (1983).
7. Resasco, D. E., and Haller, G. L., *J. Catal.* **82,** 279 (1983).
8. Tauster, S. J., and Fung, S. C., *J. Catal.* **55,** 29 (1978).
9. Wang, H.-L. *et al., in* "Metal-Support and Metal-Additive Effects in Catalysis" (B. Imelik *et al.*, Eds.), p. 19. Elsevier, Amsterdam, 1982.
10. Menon, P. G., and Froment, G. F., *in* "Metal-Support and Metal-Additive Effects in Catalysis" (B. Imelik, *et al.*, Eds.), p. 171. Elsevier, Amsterdam, 1982.
11. Tatarchuk, B. J., and Dumesic, J. A., *J. Catal.* **70,** 308, 335 (1981).
12. Guinier, A. *et al.*, "Small-Angle Scattering of X-Rays." Wiley, New York, 1955.
13. Glatter, O., and Kratky, O. (Eds.), "Small-Angle X-Ray Scattering." Academic Press, New York, 1982.
14. Goodisman, J., and Brumberger, H., *J. Appl. Crystallogr.* **4,** 347 (1971).
15. Goodisman, J., Brumberger, H., and Cupelo, R., *J. Appl. Crystallogr.* **14,** 305 (1981).
16. Kratky, O., Porod, G., and Skala, Z., *Acta Phys. Austriaca* **13,** 76 (1960).

17. Debye, P., Anderson, H. R., Jr., and Brumberger, H., *J. Appl. Phys.* **28,** 679 (1957).
18. Whyte, T. E., Jr., Kirklin, P. W., Gould, R. W., and Heinemann, H., *J. Catal.* **25,** 407 (1972).
19. Jenkins, R. G. *et al., Carbon* **20,** 185 (1982).
20. Somorjai, G. A. *et al., in* "Small-Angle X-Ray Scattering" (H. Brumberger, Ed.), p. 449. Gordon & Breach, New York, 1967.
21. Baker, R. T. K., Prestridge, E. B., and Garten, R. L., *J. Catal.* **56,** 390 (1979).
22. Lehn, J. M., Sauvage, J. P., and Ziessel, R., *Nouv. J. Chim.* **5,** 291 (1981).
23. Hartley, F. R., "Chemistry of Platinum and Palladium," pp. 168, 269. Halsted Press, New York, 1973.
24. Ginzburg, S. J. *et al.,* "Analytical Chemistry of Platinum Metals," p. 96. Wiley, New York, 1975.
25. Satterfield, C. N., "Heterogeneous Catalysis in Practice," pp. 215, 219. McGraw–Hill, New York, 1980.
26. Slichter, C. P., *Surface Sci.* **106,** 382 (1981).
27. Isaacs, B. H., and Peterson, E. E., *J. Catal.* **77,** 43 (1982), and references therein.
28. Robertson, S. D., *et al., J. Catal.* **37,** 424 (1975).
29. Sen, P., M.S. Thesis, Department of Chemical Engineering and Materials Science, Syracuse University, 1983.
30. Levy, R. B., and Boudart, M., *J. Catal.* **32,** 304 (1974).
31. Huizinga, T., and Prins, R., *in* "Metal-Support and Metal-Additive Effects in Catalysis" (B. Imelik *et al.,* Eds.), p. 11. Elsevier, Amsterdam, 1982.
32. Haller, G. L., *et al.,* private communication (1983).
33. Herrmann, J.-M., Disdier, J., and Pichat, P., *in* "Metal-Support and Metal-Additive Effects in Catalysis" (B. Imelik *et al.,* Eds.), p. 27. Elsevier, Amsterdam, 1982.
34. Short, D. R., *et al., J. Catal.* **82,** 299 (1983).